

# Calculating the distribution of transferred hyperfine fields at the Sn site in tetragonal CeScSi-type RMgSn compounds

N. R. Lee-Hone · P. Lemoine · D. H. Ryan · B. Malaman ·  
A. Vernière · G. Le Caër

© Springer Science+Business Media Dordrecht 2013

**Abstract** We present a simple model based on an isotropic transferred hyperfine field to calculate the transferred hyperfine field distribution at the Sn site of the antiferromagnetic CeScSi-type RMgSn compounds. The calculations correctly reproduce the main features observed in NdMgSn, TbMgSn, DyMgSn, HoMgSn, and ErMgSn. The transferred hyperfine field distributions are remarkably sensitive to the complex magnetic structures in the RMgSn compounds, and can be used to discriminate between competing magnetic structure models.

**Keywords** Magnetic structure · Hyperfine field distributions ·  $^{119}\text{Sn}$  Mössbauer spectroscopy

## 1 Introduction

The antiferromagnetic CeScSi-type RMgSn compounds [1, 2], where R is a rare-earth element, crystallise in the  $I4/mmm$  structure (space group No. 139). Many of these compounds have been studied by neutron powder diffraction, and show a rich variety of

---

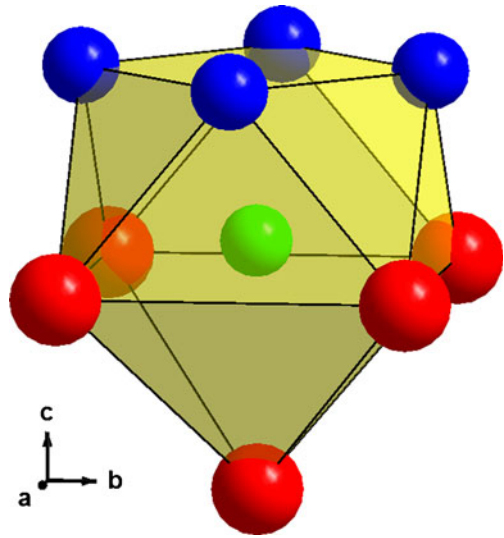
Proceedings of the 32nd International Conference on the Applications of the Mössbauer Effect (ICAME 2013) held in Opatija, Croatia, 1-6 September 2013

N. R. Lee-Hone (✉) · D. H. Ryan  
Physics Department and Centre for the Physics of Materials, McGill University,  
3600 University Street, Montreal, Quebec, H3A 2T8, Canada  
e-mail: nicholas.lee-hone@mail.mcgill.ca

P. Lemoine · B. Malaman · A. Vernière  
Institut Jean Lamour, dept P2M, équipe 103, CNRS (UMR 7198),  
Université de Lorraine, Faculté des Sciences et Technologies,  
B.P. 70239, 54506 Vandoeuvre-lès-Nancy Cedex, France

G. Le Caër  
Institut de Physique de Rennes, UMR UR1-CNRS 6251,  
Université de Rennes I, Campus de Beaulieu,  
35042 Rennes Cedex, France

**Fig. 1** Nearest neighbours of Sn. From top to bottom, the four Mg atoms (*blue*) form a square above the central Sn atom (*green*), and the five R atoms (*red*) form an inverted pyramid below



magnetic structures. At 2 K, NdMgSn adopts a simple commensurate antiferromagnetic structure [3, 4]. TbMgSn adopts either an incommensurate sine-wave modulated magnetic structure [3], or an incommensurate cycloidal spiral magnetic structure [4]. DyMgSn, HoMgSn and ErMgSn show higher order odd integer harmonics that appear progressively with decreasing temperature suggesting that the magnetic structures evolve from pure sine-wave modulated below  $T_N$  to square-wave modulated at very low temperatures [3].

Tin does not have a magnetic moment, so any hyperfine field observed by  $^{119}\text{Sn}$  Mössbauer spectroscopy is induced by either an external applied magnetic field or a magnetic field produced by a neighbouring atom [5, 6]. In the RMgSn compounds, the Sn atom is surrounded by five rare-earth atoms, as shown in Fig. 1, and the rare-earth magnetic moments induce a transferred hyperfine field at the Sn site. Fits to the  $^{119}\text{Sn}$  Mössbauer spectra of RMgSn frequently require a complex distribution of hyperfine fields. Each magnetic structure has a different transferred hyperfine field distribution (THFD), suggesting that the rare-earth magnetic structure is observable in the distributions. It should therefore be possible to use  $^{119}\text{Sn}$  Mössbauer spectroscopy to confirm the neutron diffraction results.

This paper presents a simple model based on an isotropic transferred hyperfine field that can correctly reproduce the main features of experimental  $^{119}\text{Sn}$  Mössbauer hyperfine field distributions. The distributions are remarkably sensitive to the complex magnetic structures in the RMgSn compounds, and can be used to discriminate between competing magnetic structure models.

## 2 Experimental methods

### 2.1 $^{119}\text{Sn}$ Mössbauer spectroscopy

$^{119}\text{Sn}$  Mössbauer spectra were collected in transmission mode on a constant-acceleration spectrometer using a  $\text{Ba}^{119\text{m}}\text{SnO}_3$  source ( $\sim 10$  mCi) with the sample in a helium flow cryostat. A  $25\ \mu\text{m}$  Pd foil was used to absorb the  $\text{Sn-K}\alpha$  x-rays also emitted by the source. The spectrometer was calibrated with a 25 mCi  $^{57}\text{CoRh}$  source and  $\alpha\text{-Fe}$  at room temperature.

The magnetically split spectra were analysed by a constrained Hesse-Rübartsch method [7]. This method extracts a hyperfine magnetic field distribution  $P(B)$  from an experimental spectrum, where  $P(B)\Delta B$  represents the fraction of tin atoms whose field is between  $B$  and  $B + \Delta B$ . To obtain  $P(B) (\geq 0)$ , the spectrum is considered to be a sum of  $N$  sextets of Lorentzian lines with a full-width at half-maximum  $\Gamma$  of 0.6 mm/s, characteristic of the  $^{119}\text{Sn}$  isotope. The calculated distribution is thus a histogram of  $N$  bins of identical widths  $\Delta B \sim 0.15 - 0.20$  T. It is normalized so that  $\sum_{i=1}^N P(B_i)\Delta B = 1$ , with  $B_i = (i - 1/2)\Delta B$  ( $i = 1, \dots, N$ ).

## 2.2 Transferred hyperfine field calculation

Calculation of the transferred hyperfine field distribution at the Sn site requires a full description of the magnetic structure, which can be obtained from neutron diffraction measurements. The method presented below requires as input the lattice parameters, the position of the rare-earth atom in fractional coordinates,  $z_R$ , the position of the tin atom in fractional coordinates,  $z_{\text{Sn}}$ , the basis functions for the magnetic structure,  $\mathbf{S}_j^k$ , the magnetic phase of each rare-earth atom,  $\phi_j$ , and the propagation vector,  $\mathbf{k}$ .

We first calculate the position of the rare-earth and tin atoms from the crystallographic parameters and symmetries of the  $I4/mmm$  space group. There are four R atoms per unit cell, which are located at positions  $\mathbf{R}_1 = (1/2, 1/2, 1/2 - z_R)$ ,  $\mathbf{R}_2 = (0, 0, z_R)$ ,  $\mathbf{R}_3 = (0, 0, -z_R)$ , and  $\mathbf{R}_4 = (1/2, 1/2, 1/2 + z_R)$ . The four Sn atoms are located at positions  $\text{Sn}_1 = (1/2, 1/2, 1/2 - z_{\text{Sn}})$ ,  $\text{Sn}_2 = (0, 0, z_{\text{Sn}})$ ,  $\text{Sn}_3 = (0, 0, -z_{\text{Sn}})$ , and  $\text{Sn}_4 = (1/2, 1/2, 1/2 + z_{\text{Sn}})$ . Since the Mg atoms do not carry a magnetic moment, their positions are ignored. The magnitude and direction of the rare-earth magnetic moment on atom  $j$  in unit cell  $l$  is determined by:

$$\mathbf{m}_{lj} = \sum_{\mathbf{k}} \mathbf{S}_j^k \exp(-2\pi i \mathbf{k} \cdot \mathbf{R}_l) \tag{1}$$

where  $\mathbf{S}_j^k$  are the basis functions as described by Rodríguez-Carvajal and Bourée [8].

To increase the computation speed, and to make it easier to input complex magnetic structures, we introduced the function  $F(\mathbf{R}_l, \phi_j)$  that describes the relation between the magnetic moment  $\mathbf{m}_{lj}$  and the equivalent moment in the zero-cell,  $\mathbf{m}_{0j}$ . Equation 1 then becomes:

$$\mathbf{m}_{lj} = \sum_{\mathbf{k}} \mathbf{S}_j^k F_{\mathbf{k}}(\mathbf{R}_l, \phi_j) \tag{2}$$

The computation of a sine-wave modulated magnetic structure, which is normally described by the  $\mathbf{k}$ -vector pair  $(\mathbf{k}, -\mathbf{k})$  with (1), is then reduced to:

$$F(\mathbf{r}_j, \phi_j) = \text{SineWave}(\mathbf{R}_l, \phi_j) = \cos[-2\pi(\mathbf{R}_l \cdot \mathbf{k} + \phi_j)] \tag{3}$$

$$\mathbf{m}_{lj} = \mathbf{S}_j^k \cos[-2\pi(\mathbf{R}_l \cdot \mathbf{k} + \phi_j)] \tag{4}$$

For a square-wave modulated magnetic structure, (1) requires a sum over all odd-integer harmonics of the  $\mathbf{k}$ -vector, which is computationally impractical. With (2), the infinite sum is simply replaced with

$$F(\mathbf{r}_j, \phi_j) = \text{SquareWave}(\mathbf{R}_l, \phi_j) = \text{sign}[\cos[-2\pi(\mathbf{R}_l \cdot \mathbf{k} + \phi_j)]] \tag{5}$$

$$\mathbf{m}_{lj} = \mathbf{S}_j^k \text{sign}[\cos[-2\pi(\mathbf{R}_l \cdot \mathbf{k} + \phi_j)]] \tag{6}$$

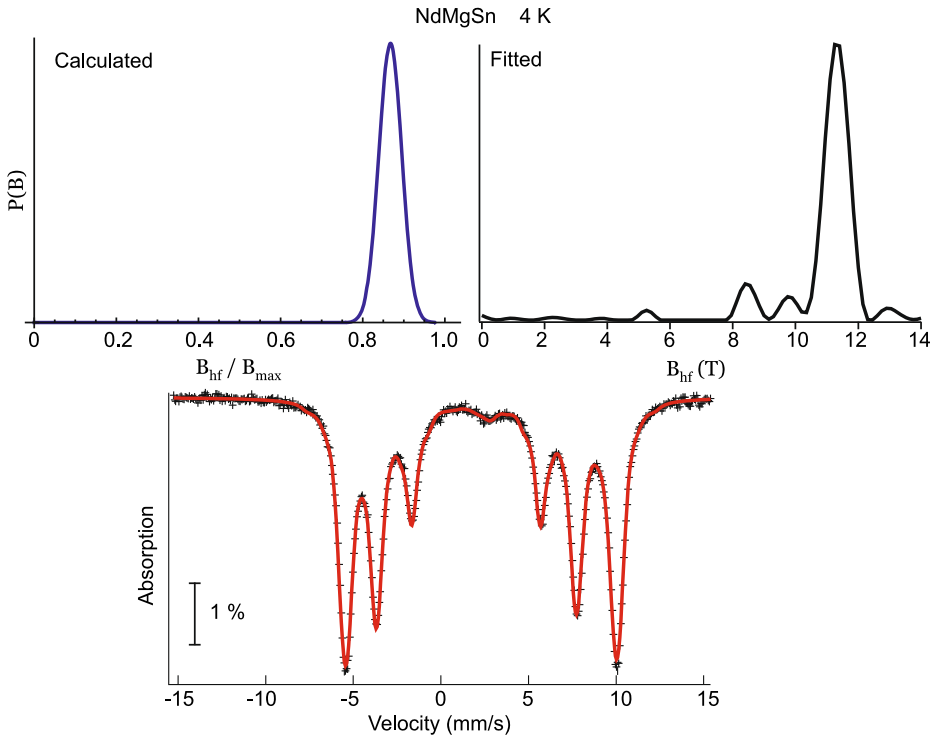


**Fig. 2** *Top left* Calculated THFD assuming a commensurate antiferromagnetic structure. *Top right* Fitted THFD of NdMgSn obtained from the  $^{119}\text{Sn}$  Mössbauer spectrum of NdMgSn at 4 K. *Bottom*  $^{119}\text{Sn}$  Mössbauer spectrum of NdMgSn at 4 K and fit to the data (solid red line)

To ensure that the descriptions of the magnetic structures with (2) are correct, we generated pictures of the moment arrangement, and compared them to pictures generated with the FPStudio program, which is part of the FullProf suite [9]. We found full agreement between our method and the output of FPStudio.

To calculate the transferred hyperfine field at a given Sn atom, the five nearest-neighbour rare-earth atoms are first selected. Their magnetic moments are then generated from (2), with a small Gaussian broadening added to smooth out the final transferred hyperfine field distribution, and the norm of the vector sum is calculated:

$$B_{hf}^{Sn} \propto \left\| \sum_{nn} \mathbf{m}_j \right\| \tag{7}$$

Repeating the calculation of  $B_{hf}^{Sn}$  over multiple units cells (over 100000) ensures that there is adequate sampling to allow for the incommensurate propagation vectors found in RMgSn compounds. As there is no way to set an absolute scale for  $B_{hf}^{Sn}$ , we instead normalize the values against the maximum transferred hyperfine field:  $B_{hf}^{Sn}/B_{max}$ . The transferred hyperfine fields are binned, and the bin height is normalised to obtain the final transferred hyperfine field distribution.

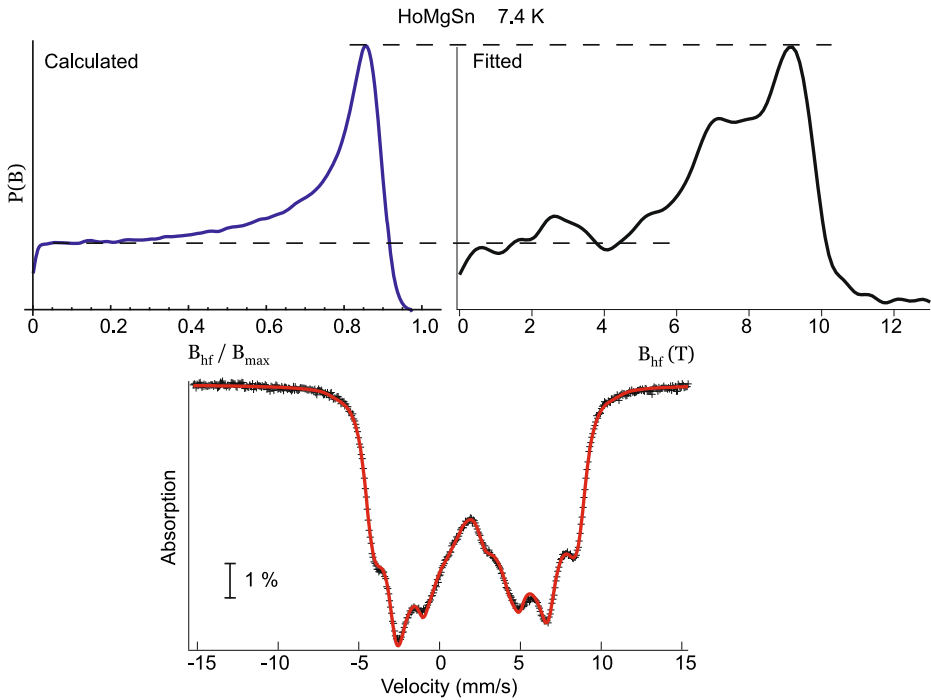


**Fig. 3** *Top left* Calculated THFD assuming a magnetic structure showing the first and third harmonics of the  $\mathbf{k}$ -vector as described in the text. *Top right* Fitted THFD of HoMgSn obtained from the  $^{119}\text{Sn}$  Mössbauer spectrum of HoMgSn at 7.4 K. The *dashed lines* emphasise that the plateau height is the same in the calculated and fitted patterns. *Bottom*  $^{119}\text{Sn}$  Mössbauer spectrum of HoMgSn at 7.4 K and fit to the data (*solid red line*)

### 3 Results

NdMgSn adopts a commensurate antiferromagnetic structure at 2 K with  $\mathbf{k} = [0, 0, 1]$ . The Nd moments are either canted by  $\theta = 65^\circ$  from the  $c$ -axis [3] or lie in the  $ab$ -plane ( $90^\circ$  from the  $c$ -axis)[4]. The  $++--$  stacking arrangement gives magnetic phases of 0, 0, 0.5, and 0.5 to  $R_1$ ,  $R_2$ ,  $R_3$ , and  $R_4$ , respectively [3]. These phases make all five rare-earth magnetic moments around a particular Sn atom point in the same direction. The THFD calculation was performed twice; once with the moments oriented  $65^\circ$  from the  $c$ -axis and once with the moments  $90^\circ$  from the  $c$ -axis. In both cases the calculated distribution shows a single peak, consistent with the fitted distribution for NdMgSn, as shown in Fig. 2. The small fluctuations in the fitted distribution are most likely due to the instability of the fitting procedure, and have no physical significance.

The THFD calculation works for the simple antiferromagnetic case, so we now explore the more complex magnetic structures observed in HoMgSn. Fits to the neutron diffraction data of HoMgSn [3] found that, at 8 K, the moments are oriented in the  $ab$ -plane with  $\phi = 67^\circ$ , and the fundamental and third harmonics are observed with  $\mathbf{k} = [0.817, 0, 0]$ . Figure 3 shows the calculated and fitted transferred hyperfine field distributions of HoMgSn at 7.4 K. The THFD calculation was performed with the fundamental and third harmonics,

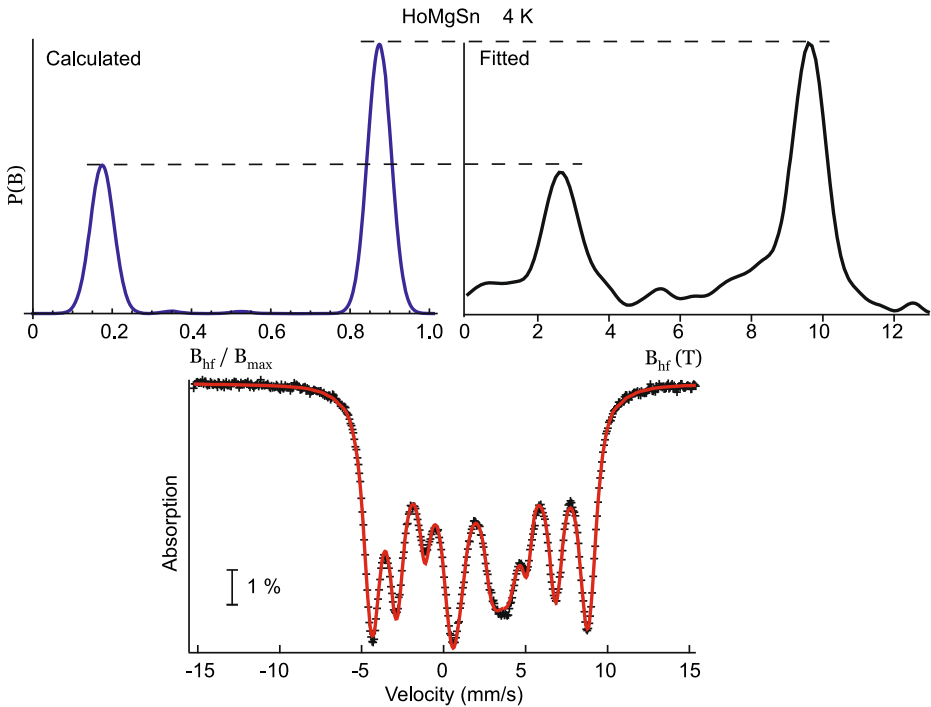


**Fig. 4** *Top left* Calculated THFD assuming a square-wave modulated magnetic structure as described in the text. *Top right* Fitted THFD of HoMgSn obtained from the  $^{119}\text{Sn}$  Mössbauer spectrum of HoMgSn at 4 K. The dashed lines emphasise that the peak heights are the same in the calculated and fitted patterns. *Bottom*  $^{119}\text{Sn}$  Mössbauer spectrum of HoMgSn at 4 K and fit to the data (solid red line)

and is characterised by a plateau with 1/4 the intensity of the main peak. A similar plateau is observed in the fitted THFD in Fig. 3.

Upon further cooling, the magnetic structure of HoMgSn evolves towards a square-wave modulated magnetic structure. At 2 K, the fifth harmonic is observed, and the moments orient in the  $ab$ -plane with  $\phi = 50^\circ$ , and  $\mathbf{k} = [0.822, 0, 0]$  [3]. Figure 4 shows the fitted hyperfine field distribution of HoMgSn at 4 K, and the calculated pattern assuming a square-wave modulated magnetic structure. The fitted and calculated THFDs are in good agreement, and show two main peaks. The relative heights of the two peaks are correctly reproduced by the calculation method.

The good agreement between the calculated and fitted THFD for simple antiferromagnetic, square-wave modulated, and fundamental/third harmonic magnetic structures is a strong indication that the method is sound. We now turn to the magnetic structure of DyMgSn that is characterised at 2 K by the incommensurate propagation vector  $\mathbf{k} = [0.830, 0.014, 0]$ . The moments are oriented within the basal plane, with  $\phi = 137^\circ$ . Only the fundamental and third harmonics are observed, suggesting that the structure is not fully square-wave modulated by this temperature. However, the third harmonic peak intensities are almost indistinguishable from the background, so it is unlikely that a fifth harmonic could be observed if it were present [3].

The THFD of DyMgSn at 4 K, shown in Fig. 5, is very similar to that of HoMgSn at 4 K (Fig. 4), which was determined to be square-wave modulated. A calculation of the

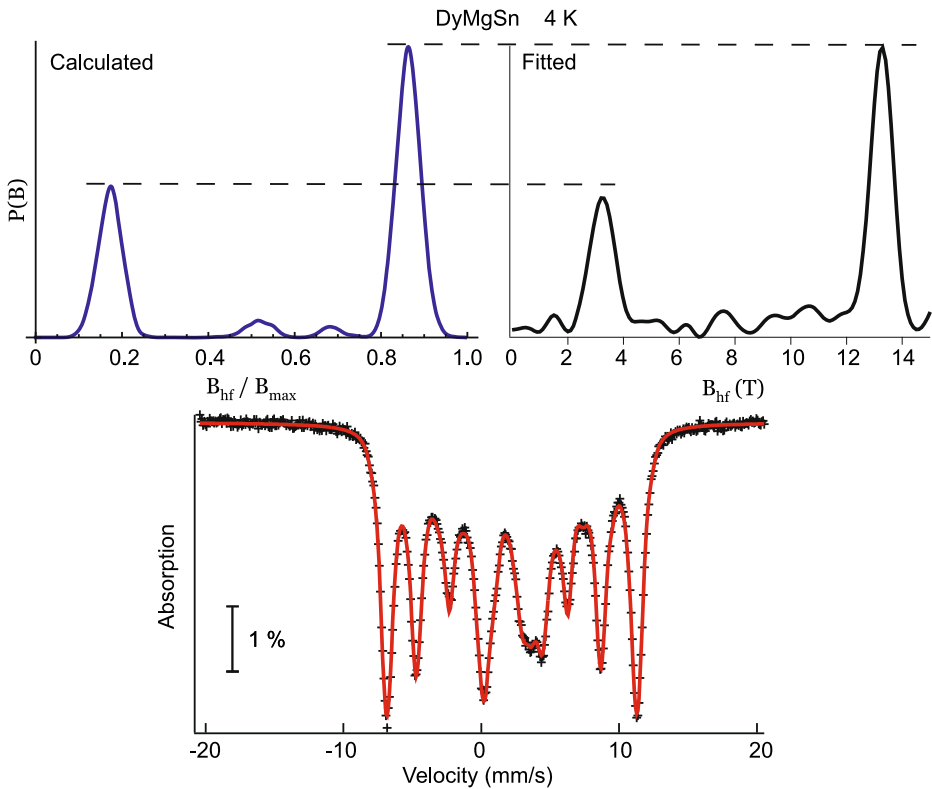


**Fig. 5** *Top left* Calculated THFD assuming a square-wave modulated magnetic structure as described in the text. *Top right* Fitted THFD of DyMgSn obtained from the  $^{119}\text{Sn}$  Mössbauer spectrum of DyMgSn at 4 K. The dashed lines emphasise that the peak heights are the same in the calculated and fitted patterns. *Bottom*  $^{119}\text{Sn}$  Mössbauer spectrum of DyMgSn at 4 K and fit to the data (*solid red line*)

THFD for DyMgSn with a square-wave modulated magnetic structure agrees well with the fitted distribution (Fig. 5). We conclude that the magnetic structure of DyMgSn is square-wave modulated below 4 K, and that the neutron powder diffraction pattern simply cannot detect the higher order harmonics necessary to confirm this. The  $^{119}\text{Sn}$  transferred hyperfine field distribution is thus more sensitive to the presence of higher-order harmonics than neutron powder diffraction. This shows that the calculation of THFDs coupled with  $^{119}\text{Sn}$  Mössbauer spectroscopy measurements can reveal supplemental magnetic structure information.

No neutron data on DyMgSn are available at temperatures above 2 K. However, it is very common for square-wave modulated magnetic structures to become sine-wave modulated at higher temperatures. With this assumption, we calculated the  $^{119}\text{Sn}$  transferred hyperfine field distribution with a simple sine-wave modulated magnetic structure. The calculated pattern is shown in the top left panel of Fig. 6, and is in good agreement with the fitted distribution of DyMgSn at 14.8 K. As with the 7.4 K pattern of HoMgSn, the main peak to plateau ratio is 4:1.

We have established that the transferred hyperfine field distribution at the Sn site in the CeScSi-type RMgSn compounds is very sensitive to its environment, and that comparing

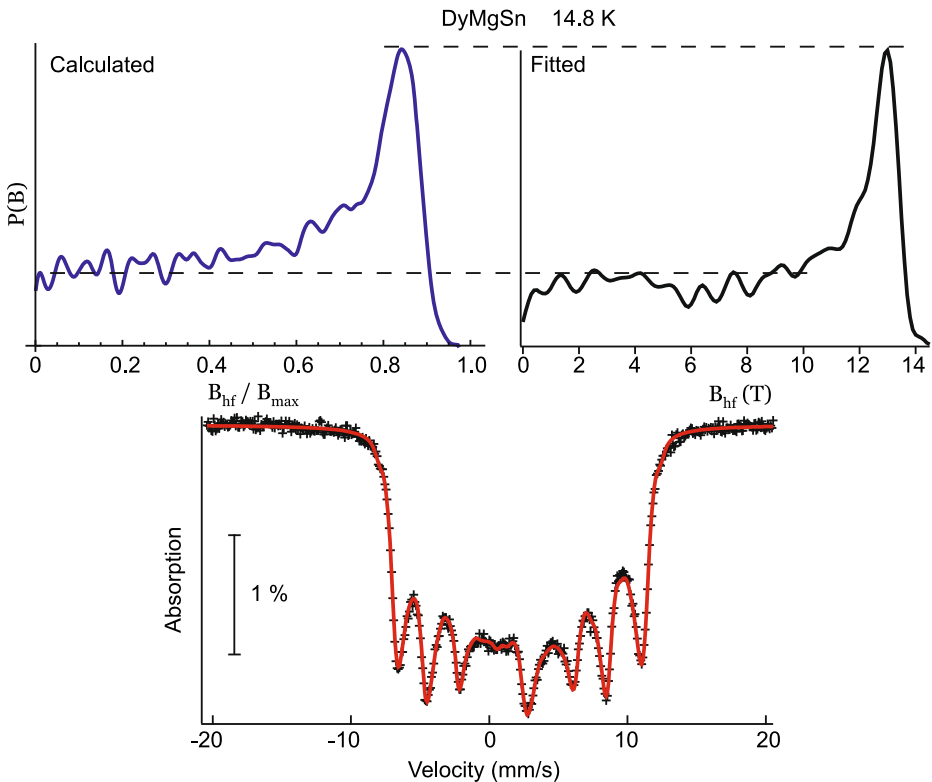


**Fig. 6** Top left Calculated THFD assuming a sine-wave modulated magnetic structure as described in the text. Top right Fitted THFD of DyMgSn obtained from the  $^{119}\text{Sn}$  Mössbauer spectrum of DyMgSn at 14.8 K. The dashed lines emphasise that the plateau height is the same in both patterns. Bottom:  $^{119}\text{Sn}$  Mössbauer spectrum of DyMgSn at 14.8 K and fit to the data (solid red line)

the fitted distribution with calculations performed with the method presented in this paper can supplement the information obtained from neutron powder diffraction.

We now examine the case of TbMgSn where two separate investigations came to different conclusions about the magnetic structure. Lemoine et al. [3] found that the magnetic structure of TbMgSn at 2 K is sine-wave modulated with  $\theta = 90^\circ$ ,  $\phi = 43^\circ$ , and  $\mathbf{k} = [0.828, 0, 0]$ . A separate study by Ritter et al. [4] found that the moments form a cycloidal spiral with the moments confined to the basal plane, with  $\mathbf{k} = [0.84, 0, 0]$ .

The fitted  $^{119}\text{Sn}$  transferred hyperfine field distribution is shown in the bottom right panel of Fig. 7, and the calculated THFDs for sine-wave modulated and cycloidal spiral magnetic structures are shown in the top left and top right panels respectively. The calculated cycloidal spiral THFD has a single peak, whereas the calculated sine-wave modulated THFD has a plateau. As no plateau is observed in the fitted THFD, the magnetic structure of TbMgSn is not purely sine-wave modulated. The cycloidal model matches the fitted THFD except for the feature around 10 T in Fig. 7. This suggests that the structure is not purely cycloidal either. The absorption peaks of the TbMgSn  $^{119}\text{Sn}$  Mössbauer spectra are broadened, indicating that there is some modulation of the  $\text{Tb}^{3+}$  magnetic moment. Hence, the  $^{119}\text{Sn}$  Mössbauer results combined with the calculated and fitted THFD indicate that the magnetic structure of TbMgSn is characterized by both a modulation of the  $\text{Tb}^{3+}$  moments

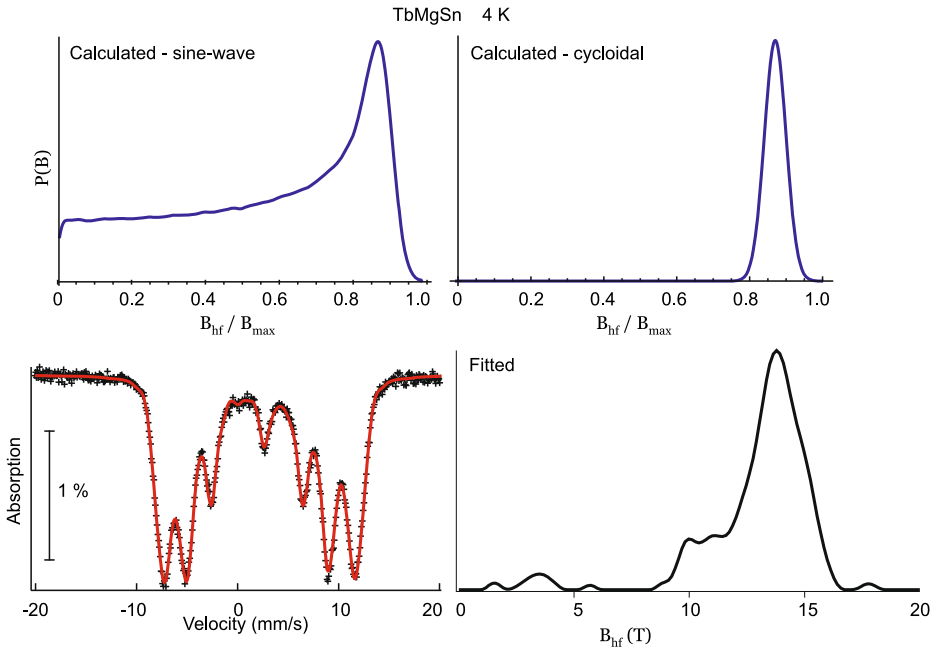


**Fig. 7** *Top left* Calculated THFD assuming an incommensurate sine-wave modulated magnetic structure. *Top right* Calculated THFD assuming an incommensurate cycloidal spiral magnetic structure. *Bottom right* Fitted THFD obtained from the  $^{119}\text{Sn}$  Mössbauer spectrum of TbMgSn at 4 K. The cycloidal spiral model in the top right panel is clearly a better match to the fitted THFD. *Bottom left*  $^{119}\text{Sn}$  Mössbauer spectrum of TbMgSn at 4 K and fit to the data (solid red line)

and a cycloidal modulation of the moment direction. This leads us to conclude that the magnetic structure of TbMgSn is elliptical.

We now turn to the case of ErMgSn where the magnetic moments are aligned with the  $c$ -axis. At 4 K, the fundamental and third harmonics are observed in the neutron diffraction pattern, with  $\mathbf{k} = [0.800(1), 0, 0]$  [3]. The calculated THFD assuming a commensurate magnetic structure with first and third harmonics is shown in the top left panel of Fig. 8. It is clearly a poor match for the fitted distribution in the bottom right panel of Fig. 8.

As neutron diffraction is a reciprocal-space technique, it is very difficult to observe minor changes in real-space periodicity such as the difference between a commensurate structure and one that is very close to commensurate. The transferred hyperfine field distribution, on the other hand, represents information about real-space. If the magnetic moment is modulated and the magnetic structure is commensurate, the modulation is sampled at discrete points, which picks out certain moment values. For a modulated magnetic moment with an incommensurate magnetic structure, the modulation is sampled at all points, and no particular values are isolated. We thus expected the calculations and fitted distributions to be different for commensurate/incommensurate magnetic structures, so we performed the transferred hyperfine field calculation for ErMgSn with  $\mathbf{k} = [0.801, 0, 0]$  (within error of the reported propagation vector). The results are shown in the top right panel of Fig. 8. The calculated THFD is clearly in agreement with the fitted one. In both cases, there is a plateau at approximately 1/2 the intensity of the main peak.

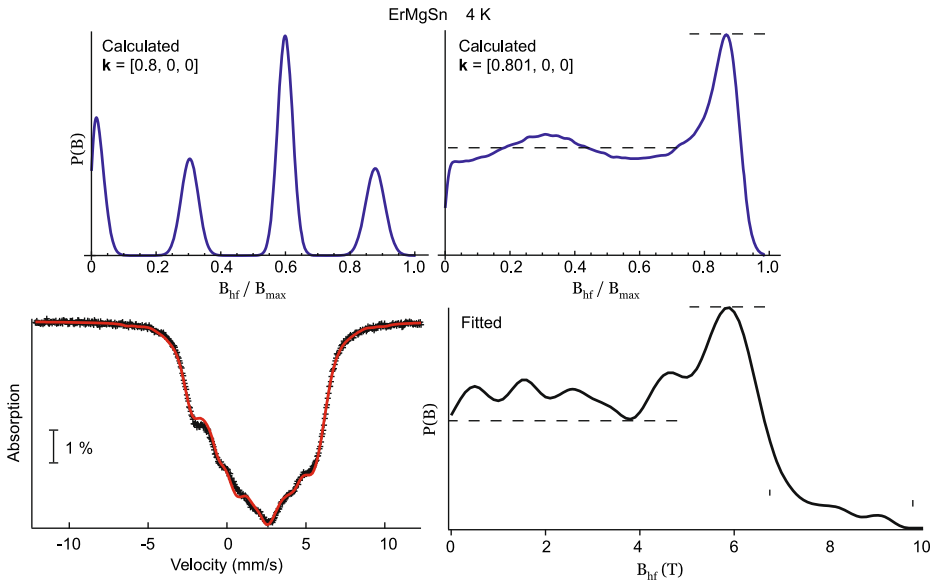


**Fig. 8** *Top left* Calculated THFD assuming a commensurate propagation vector  $\mathbf{k} = [0.8, 0, 0]$ . *Top right* Calculated THFD assuming an incommensurate propagation vector  $\mathbf{k} = [0.801, 0, 0]$ . *Bottom right* Fitted THFD obtained from the  $^{119}\text{Sn}$  Mössbauer spectrum of ErMgSn at 4 K. The incommensurate model in the top right panel is clearly a better match to the fitted THFD. *Bottom left*  $^{119}\text{Sn}$  Mössbauer spectrum of ErMgSn at 4 K and fit to the data (*solid red line*)

## 4 Conclusions

Although the detailed agreement between calculated and fitted  $^{119}\text{Sn}$  transferred hyperfine field distributions is not perfect, we have demonstrated that a simple calculation based on a vector sum of rare-earth moments reproduces the major features observed in the THFDs of CeScSi-type RMgSn compounds. The calculated THFDs for different magnetic structures are distinct. Both ErMgSn at 4 K and HoMgSn at 7.4 K have the same magnetic structure type (first and third harmonics), but the different magnetic moment arrangements and  $\mathbf{k}$ -vectors give different ratios between the plateau and main peak. In HoMgSn (Fig. 3) the ratio is 1:4, and in ErMgSn the ratio is 1:2. This indicates that the calculation method and fitted distributions are sensitive to the differences in orientation and  $\mathbf{k}$ -vector. As was shown with ErMgSn, the calculated and fitted distributions are especially sensitive to the differences between incommensurate and commensurate magnetic structures, which is not always the case with neutron diffraction. The TbMgSn case highlighted that the technique can be used to discriminate between competing magnetic structure models. Comparing transferred hyperfine field distribution calculations with  $^{119}\text{Sn}$  Mössbauer spectra can thus yield insight into magnetic structures that is not possible with neutron diffraction alone.

**Acknowledgments** Financial support for various stages of this work was provided by the Natural Sciences and Engineering Research Council of Canada and Fonds Québécois de la Recherche sur la Nature et les Technologies.

## References

1. Manfrinetti, P., Provino, A., Gschneidner, K.A. Jr.: *J. Alloy Compd.* **482**, 81–85 (2009)
2. Lemoine, P., Vernière, A., Maréché, J.F., Malaman, B.: *J. Alloy Compd.* **508**, 9–13 (2010)
3. Lemoine, P., Vernière, A., Venturini, G., Capelli, S., Malaman, B.: *J. Magn. Magn. Mater.* **324**(6), 961–976 (2012)
4. Ritter, C., Provino, A., Manfrinetti, P., Gschneidner, K.A. Jr.: *J. Alloy Compd.* **509**(41), 9724–9732 (2011)
5. Perry, L.K., Ryan, D.H., Venturini, G.: *Phys. Rev. B* **75**, 144417 (2007)
6. Le Caër, G., Malaman, B., Venturini, G., Kim, I.B.: *Phys. Rev. B* **26**, 5085 (1982)
7. Le Caër, G., Dubois, J.M.: *J. Phys. E Sci. Parasitol.* **12**(11), 1083 (1979)
8. Rodríguez-Carvajal, J., Bourée, F.: *EPJ Web of Conferences* **22**, 00010 (2012)
9. Rodríguez-Carvajal, J.: *Phys. B* **192**, 55 (1993)